

Creation of Lipid-Based Nanoparticles for the Concurrent Administration of Lapatinib and Anti-Survivin siRNA for the Treatment of HER2+ Breast Cancer

1. **Dr.sk.salma***, PROFESSOR, DEPT OF PHARMACEUTICAL CHEMISTRY,
2. **D. Mahidhar Reddy**, Asso. Professor, DEPT OF PHARMACEUTICS
3. **P. Venkata Pavani**, Asst. Professor, DEPT OF Pharmaceutical Analysis
4. **s. vijitha**, Asst. Professor, Pharmaceutical Analysis
5. **Dr.M. SREENIVASULU**, PRINCIPAL, NARAYANA PHARMACY COLLEGE
1,2,3,4,5 NARAYANA PHARMACY COLLEGE, CHINTHA REDDY PALEM, NELLORE

Abstract: Lipid-based nanoparticles (LBNP) were developed in this study to combine siRNA targeting the apoptosis inhibitor protein Survivin (siSurvivin) in an injectable form with the tyrosinekinase inhibitor (TKI) Lapatinib (LAPA). Lipid nanocapsules (LNCs) covered with a cationic polymeric shell made of chitosangrafted via a transacylation process serve as the foundation for this nanosystem. While hydrophilic siRNA is electrostatically attached to the surface of the thenanocarrier, the hydrophobic LAPA is dissolved in the interior oily core. The co-loaded LBNP has a size of 130 nm, a slightly positive zetapotential (+21 mV), and an arrow-sized distribution (polydispersity index (PDI)<0.3). At high rates of >90% (10.6 mM) and 100% (4.6 μM), respectively, LAPA and siRNA were loaded into LBNP. The human epidermal growth factor receptor 2 overexpressed (HER2+) breast cancer cell line SK-BR-3 was able to absorb the siRNA-LAPA_LBNP with ease. Furthermore, the cytotoxicity tests verified that the cells with the measured concentrations—which correspond to LAPA concentrations ranging from 1 to 10 μM—at various incubation durations up to 96 hours are not toxically affected by the blank chitosan adorned LBNP. Additionally, siSurvivin-LAPA_LBNP had a notable synergistic cytotoxic impact in comparison to siCtrl.-LAPA_LBNP, although siCtrl.-LAPA_LBNP exhibited a higher cytotoxic effect than lapatinib salt. All of these results indicated that the modified LBNP that was created would enhance the anti-Survivin siRNA and LAPA anti-cancer effects.

Keywords: lipid-basednanoparticles;co-delivery;Lapatinib;Survivin;siRNA;HER2+breastcancer

Introduction

Cancer is now the second most common cause of mortality worldwide. Breast cancer in women has surpassed lung cancer as the most common cause of cancer globally. An estimated 2.3 million new cases were reported in 2020, accounting for 11.7% of total cancer cases. With 685,000 fatalities annually, it ranks as the sixth most common cause of cancer mortality globally. Breast cancer is responsible for 1 in 4 cancer cases and 1 in 6 cancer deaths among women [1]. The receptor tyrosine kinases belonging to the epidermal growth factor receptor (EGFR) family are the most often overexpressed receptors in breast cancer cells. About 40% and 25% of breast tumours, respectively, overexpress EGFR and human epidermal growth factor receptor-2 (HER2), which are linked to aggressive tumour characteristics and a bad prognosis [2]. The advent of targeted therapies that target HER2 receptors, such as monoclonal antibodies (Mabs) like trastuzumab and pertuzumab, antibody-drug conjugates (ADCs) like trastuzumabemtansine and trastuzumabderuxtecan, and tyrosinekinase inhibitors (TKIs) like lapatinib, neratinib, tucatinib, and erlotinib, have thankfully made HER2+ breast cancer treatable in recent years [3–7]. A dual EGFR/HER2 kinase inhibitor called lapatinib has been approved for oral use in individuals with trastuzumab-resistant Breast cancer with overexpression of HER2 since 2007 [8]. Regretfully, lapatinib has inferior pharmacokinetic characteristics and is classified as a class-II medication in the biopharmaceutics categorisation system (BCS) (low solubility, high permeability). Food consumption has a major impact on its oral bioavailability, which varies greatly across patients [8,9]. Numerous studies have also shown that before LAPA is administered, the bioavailability of both high-fat and low-fat diets increases [8,9]. LAPA bioavailability is also influenced by stomach pH in addition to meal consumption. LAPA absorption is decreased by higher

stomach pH, and LAPA bioavailability is decreased by concurrent use of medications that interfere with gastric acidity [9,10]. Additionally, lapatinib is heavily linked to alpha-1 glycoprotein and plasma albumin, which lowers its systemic exposure to the tumour sites. Its clinical application is restricted due to its poor biostability, low water solubility, resistance dangers, and issues with patient compliance (dosing many tablets daily) [11,12]. The development of an intravenous injectable vectorised version of lapatinib is one possible substitute.

Current studies have also shown that, in comparison to monotherapy, combinations of gene-modulatory medicines with anti-cancer medications provide superior therapeutic results [13]. Such a combination may improve (i) the synergistic impact of each treatment modality and (ii) tumour site selectivity, while (iii) successfully reversing drug resistance [14]. Lapatinib and anti-survivin siRNA (siSurvivin) will be used in this instance. Tyrosine kinase receptor inhibition is how LAPA works, and it also contributes to the downregulation of anti-apoptotic genes like Survivin [15]. Survivin is a protein that inhibits apoptosis and has a dual function of controlling cell development and preventing death. Therefore, suppressing survivin expression may be a promising strategy to induce tumour site cell death [16–19]. Numerous drug delivery methods, such as polymer-based nanoparticles [20], lipid-based nanoparticles [21], and hybrid inorganic nanoparticles [22], have been reported and optimised to date in order to sustain the co-distribution of various treatments. By lowering side effects, increasing therapeutic effectiveness, targeting tumours, reversing medication resistance, and producing synergistic, enhanced therapeutic results, these strategies offer enormous promise in the treatment of cancer. Due to their unique properties, lipid

nanocapsules (LNCs) have drawn a lot of interest from different drug delivery methods. The phase-inversion approach serves as the foundation for their development. They are made up of an oily core and a shell made of a combination of polyethylene glycol's hydroxystearate and lecithin [23]. Exciting aspects of LNC formulations include the fact that their primary ingredients have been authorised for intravenous administration in vivo and that their development process is straightforward and basic, requiring no additional organic or hazardous solvents to achieve significant drug loading capacities. Additionally, LNCs are adaptable nanoparticles that may undergo additional alterations to improve their stability and specificity, including (i) surface functionalisation, (ii) the capacity to add various solubilising agents to improve the effectiveness of encapsulating medications with poor solubility profiles, and (iii) their compatibility with other therapeutic approaches [24–28]. Additionally, it has been shown that LNCs may be utilised to deliver lipophilic chemotherapeutics and siRNA all at once [29–31].

Our current work offers a thorough, in-depth method for creating a parenteral version of anti-Survivin siRNA with lapatinib as a therapy option for HER2+ breast cancer. To enhance the therapeutic efficacy of LAPA, multifunctional lipid-based nanoparticles (LBNP) were created to co-deliver LAPA and anti-Survivin siRNA. In order to achieve this, LAPA-loaded LNCs (LAPA_LNCs) were made using the solubility enhancer Labrasol® to encapsulate LAPA in the oily core. LAPA_LNCs were then surface modified with chitosan through a transacylation reaction between the pegylated hydroxystearate and the functional amino groups of chitosan to create LAPA_LBNP [32,33]. To create siRNA-LAPA_LBNP, negatively charged siRNA was then electrostatically loaded onto positively charged LBNP. The size, surface charge, polydispersity index (PDI), and LAPA encapsulation of the produced LBNPs have all been determined. efficiency, storage stability, and siRNA complexation. They were then evaluated in vitro to examine their cytotoxicity and cellular absorption.

1. Results and Discussion

Formulation of LAPA_LBNP

A phase inversion temperature approach was used to create LAPA_LNCs [23, 25]. Figure 1 shows a schematic representation of the formulation process. Lapatinib was, in short, dissolvable in Labrasol® as a solubility enhancer, followed by the addition of Labrafac®WL1349, Kolphor®HS15, Lipoid®S75-3, NaCl, and water. Between 85 °C and 45 °C, three progressive heating and cooling cycles were conducted. 2 °C deionised water was added to the mixture during the previous cooling cycle's inversion phase (61–63 °C). Following surface modification by a transacylation process, low molecular weight chitosan oligosaccharide (5 kDa) was grafted onto LAPA_LNCs to create LAPA_LBNP [33]. By applying the cationic chitosan polymer to the nanoparticles, siRNA was able to adsorb via electrostatic interactions, forming siRNA-LAPA_LBNP (Figure 1). In order to be included into the core of the LNC, lapatinib, a tiny molecule with a very poor water solubility at 25°C (7µg/mL), was first dissolved with the aid of a solubility enhancer called Labrasol®. When Labrasol®, a lipid-based

excipient, comes into contact with water, it may self-emulsify and create microemulsions with only a little stirring. However, the kind and concentration of oils and co-surfactants utilised determine how well it creates these microemulsions [25,34,35]. Because of Labrasol®'s placement near the interface and its capacity to bind water molecules, Libster et al. claim that its presence in the lipid-water system may result in reorganisation in the structure of produced liquid crystals, which is shown by a reduction in the system's elasticity [36]. Due to the Tyndall effect, the final formulations of LNCs and LAPA_LNCs had blue reflection and were opalescent white and weak yellow, respectively. Because of its high transformation efficiency and low toxicity when compared to other polymers, such polyethyleneimine (PEI), chitosan polymer has been the subject of much research in nanotechnology and is often a good choice. Its inability to dissolve well in neutral environments and the formation of large nanoparticles when a high molecular weight version of chitosan is utilised are its main drawbacks [37]. Recent research has shown that chitosan-based nano-delivery systems may assist in removing obstacles to the medication's distribution to the intended recipient, hence enhancing the therapeutic effectiveness of the medication [38]. A byproduct of chitosan degradation, chitosan oligosaccharide lactate has recently acquired favour because of its improved water solubility and usefulness as an analogue carrier [39–41]. Because of the amine groups' nature, chitosan exhibits positive charges that vary according to the pH of the solvent. This enables stable complexes to form via electrostatic interactions with negatively charged molecules like nucleic acids. Enhancement of Chitosan LBNP Designing LBNP with reasonable physicochemical characteristics that may co-load a siRNA and LAPA payload that is high, which is advantageous for improved cytotoxicity and more cellular uptake. Three distinct chitosan concentrations—referred to as 1×, 2×, and 3×—were used to assess siRNA complexation into LBNP. Each formulation's size ranged from 120 to 150 nm, and its positive surface charge ranged from +20 to +30 mV (Figure S1). Furthermore, throughout the 28-day testing period, the zeta potential values varied, but the size and PDI measurement results were near to one another. Zeta potential measurements in the 3× chitosan formulation exhibit a diminishing trend from day 0 to day 28, dropping from about +30 mV to +10 mV (Figure S1). Figure 2 displays the outcome of the agarose gel electrophoresis. In order to assess the quantity of free and total siRNA in the formulations, the three siRNA_LBNP formulations (chitosan 1×, 2×, and 3×, siRNA concentration 4.6 µM) were compared to free siRNA. Each sample was examined in the presence and absence of heparin. Since there is a noticeable fluorescent band when heparin is not present, the 1× and 2× LBNP formulations were unable to effectively complex the whole quantity of siRNA. It goes without saying that the 3× LBNP formulation might make the siRNA adequately, as hardly little fluorescence is seen when heparin is not present. The result shown that a virtually full siRNA complexation would be produced by 1.8 mg/mL of chitosan (or 3×) in the formulation. All formulations had fluorescent bands that were as strong as those of free siRNA when heparin was present. This suggests that throughout the formulation process, siRNA was not altered. These findings led us to choose a 3×LBNP formulation for the ensuing cellular assessments and physicochemical characterisation.

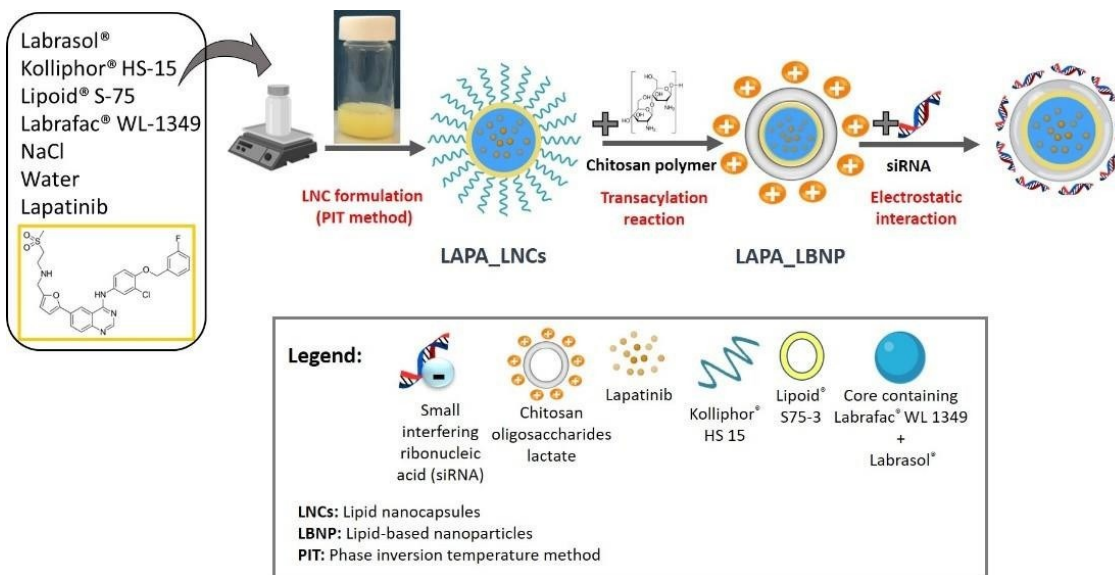


Figure1. Schematic illustration of the siRNA-LAPA_LBNP formulation process.

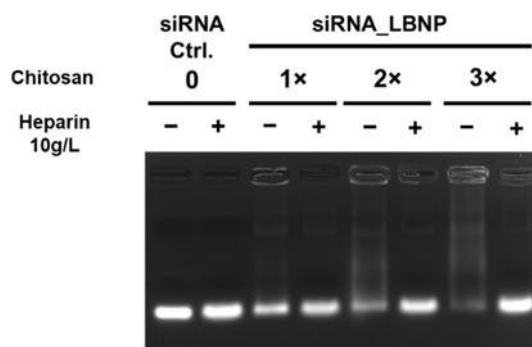


Figure2. Gel retardation assay image demonstrating the siRNA protection in the modified lipid-based nanoparticles with different chitosan concentrations after formulation (day 0). The initial theoretical chitosan concentration of 0.6 mg/mL is 1×, while the double and triple chitosan concentrations are 2× and 3×, respectively. siRNA formulated in LBNP in the presence (+) or absence (-) of heparin was compared to naked siRNA. Lanes without heparin show free siRNA amount, and lanes with heparin show total siRNA amount in the sample.

Characterization of LBNP

Based on dynamic light scattering experiments (Table 1), blank LNCs had a narrow PDI of 0.116 ± 0.023 and an average particle size of 86.9 ± 12.9 nm. The blank LNCs had a zeta potential of around -4.15 ± 4.35 mV. Because of the PEG shell provided by Kolliphor® HS15, the surface charge of blank LNCs is neutral or somewhat negative [36]. Following chitosan layer surface modification, dialysis-based purification, and pH adjustment to load siRNA, the LAPA_LBNP's size grows to 126.9 ± 20.6 nm, with a zeta potential of $+28.42 \pm 6.69$ mV and a PDI of 0.145 ± 0.080 . The efficient chitosan grafting at the NPs' surface is explained by the size increase. A naturally occurring linear polymer of glucosamine and acetylglucosamine is chitosan, which, because of the protonation-deprotonation balance of its amino groups at varying pH values, functions as a pH-responsive polymer and behaves as a polyelectrolyte with positive charge density at low pH [42–44]. Their

protonation in acidic conditions is the cause of the positive surface charge. With a homogeneous mono dispersion distribution of around 0.09 ± 0.052 , siRNA loading caused the size of co-loaded nanoparticles to decrease to 123.94 ± 17.10 nm, suggesting that the siRNA integration in the chitosan layer caused a minor but non-significant shrinkage in the NP's size. With a reduced PDI of less than 0.1, a high monodispersity was effectively produced. This was intriguing since formulations using electrostatic self-assembly often cannot achieve this low value. The siRNA-LAPA_LBNP nanoparticles' surface charge dropped to $+20.84 \pm 8.67$ mV as expected, demonstrating that the polymer-positive amino groups and siRNA-negative phosphate groups successfully electrostatically loaded (Table 1). Reasonable colloidal stability was established by the PDI of less than 0.3 for all of the formulations.

Table 1. Mean particle size, polydispersity index, and zeta potential of the LNCs, LAPA_LNCs, LAPA_LBNP, and siRNA-LAPA_LBNP.

Formulation	DH (nm)	PDI	ZetaPotential(mV)	EE (%)
LNCs	86.9±12.9	0.116±0.02	-4.15±4.35	-
LAPA_LBNP	126.9±20.60	0.14±0.08	+28.42±6.69	94.51±6.63
siRNA-LAPA_LBNP	123.9±17.10	0.09±0.05	+20.84±8.67	

D_H: Hydrodynamic diameter, EE: Encapsulation efficiency, PDI: Polydispersity index, LAPA: Lapatinib, LBNP: Lipid-based nanoparticles, LNCs: lipid nanocapsules, mV: millivolt.

To make sure that the LAPA concentration is maintained throughout the whole formulation process of LBNP, LAPA encapsulation efficiency experiments were conducted following various formulation processes. As shown in Table 1, LAPA_LBNP had an experimental drug payload of 5.5–6.3 mg of LAPA per gramme of LNC solution (9.5 mM–10.9 mM) and an EE of 94.51±6.63%. The formulation's potential for parenteral delivery is shown by its extremely high loading capacity for a poorly soluble molecule like LAPA. In contrast to the expected value of 0.247 ±0.005 mg/mL, Buss et al. created micelles with a total lapatinib concentration of 98.77 ±2.01% [45].

Gel electrophoresis was then used to evaluate siRNA_LBNP and siRNA-LAPA_LBNP, which were made with 3×chitosan and siRNA concentration 4.6µM (Figure 3). Free siRNA serves as a control and exhibits a strong fluorescence signal both with and without heparin. Since there was no free siRNA, LBNP without siRNA did not exhibit a fluorescence signal. However, since LBNP and LAPA were present, there were

two faint or strong fluorescence bands on top of the gel for blank LBNP and LAPA_LBNP, respectively. Numerous publications showed that since LAPA is hydrophobic, it may act as a "turn-on" fluorophore by causing fluorescent aggregates to form in solution. UV can detect the spectroscopically different photoemission that results from the interaction between the proteins and the lipid carrier [46]. There is some free siRNA in the formulation since siRNA_LBNP and siRNA-LAPA_LBNP exhibit strong fluorescence bands at the siRNA level when heparin is present and a weak fluorescence signal when heparin is not. The findings for blank LBNP and LAPA_LBNP were consistent with the fluorescence signal at LAPA and LBNP levels. According to these findings, siRNA_LBNP and siRNA-LAPA_LBNP may eventually entrap the siRNA. Furthermore, the siRNA complexation into LBNP was not disrupted by LAPA encapsulation. Up to 4.6µM of the siRNA may be loaded into their polymer layer using our LBNPs.

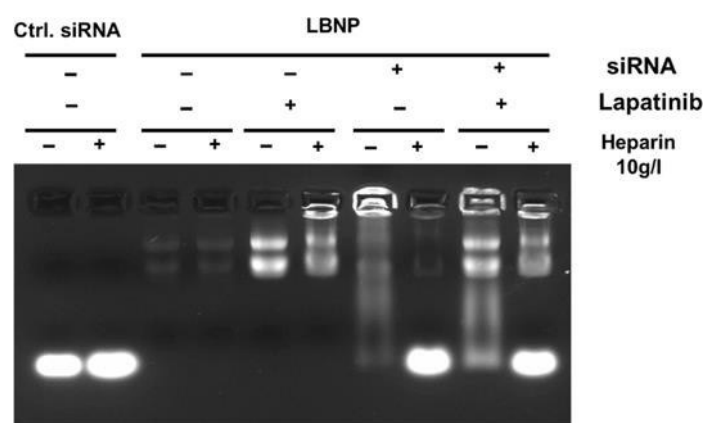


Figure 3. Gel retardation assay image demonstrates siRNA protection in the modified lipid-based nanoparticles. Control siRNA formulated in blank or Lapatinib loaded LBNP in the presence (+) or absence (-) of heparin were compared to naked siRNA. Lanes without heparin show free siRNA amount, and lanes with heparin show total siRNA amount in the sample.

Briefly, 125 nm-sized nanoparticles with a positive surface charge were created. Both size and surface charge are known to have a significant impact on the destiny of nanoparticles, contributing to factors such as serum stability, charge-mediated cellular uptake, and possible in vivo contact with the negatively charged tumour cell membrane [47–50]. The particle diameter should ideally fall between 10 and 150 nm for such efficient penetration, as this will support a longer circulation period and greater accumulation at the target site. Furthermore, compared to neutral and negatively charged

NPs, positively charged NPs exhibit superior absorption via direct penetration [51]. The NPs used in this work have physicochemical properties that make them appropriate for intravenous delivery. They can encapsulate siRNA on the surface for up to 100% (4.6 µM) and LAPA at the core interface for up to 90% efficiency (~6.3 mg/g; 10.6 mM). Additionally, via charge-mediated absorption, the positive surface charge may improve NP cellular delivery. Stability of Storage for siRNA_LBNP During the 28-day testing period, storage stability was

examined. Indicating that the original nanoparticles did not experience major changes, retained their dimensions and homogeneity, and retained their surface modification characteristics, physical appearance, size, PDI, and zeta potential values should be at their best over the research period. The nanoparticulate system's potential in vivo use and the prediction of the nanoparticles' destiny within the biological system depend on its physical and storage stability [52]. Consequently, two separate experiments were conducted. The first was to verify LBNP stability and determine if siRNA loading depends on the formulation's age; the second examined the properties of siRNA_LBNP over time in relation to a physical combination of chitosan and siRNA (=polyplexes). For all trials, the formulations seemed identical optically, showing no obvious indications of instability, such as flocculation or coalescence.

In the first experiment, siRNA was introduced at various intervals prior to characterisation after LBNP was made with

an optimised chitosan concentration of 1.8 mg/mL (Figures 4 and S2). Low PDI values and stable particle sizes were observed across time (Figure 4A). After seven days of stability, the zeta potential values (Figure 4B) decreased from day seven to day twenty-eight without any discernible siRNA release (Figure S2). The findings suggest that siRNA loading may occur at any time within the first seven days after LBNP formulation. The pH shift of the suspension over time may have an impact on the ionic strength or any chemical balance in the suspension, which might account for the surface charge decrease between days 7 and 28 [53,54]. The pegylated surface's steric hindrance is primarily responsible for LNC stability. For almost six months of storage, blank, unmodified LNCs demonstrated stability in size, PDI, and zeta potential values with extremely low variation of the values that were measured (data not displayed). Compared to LNCs, LBNP formulations shown larger volatility in the observed values. This could result from the chitosan polymer dislodging the PEG molecules after the transacylation step.

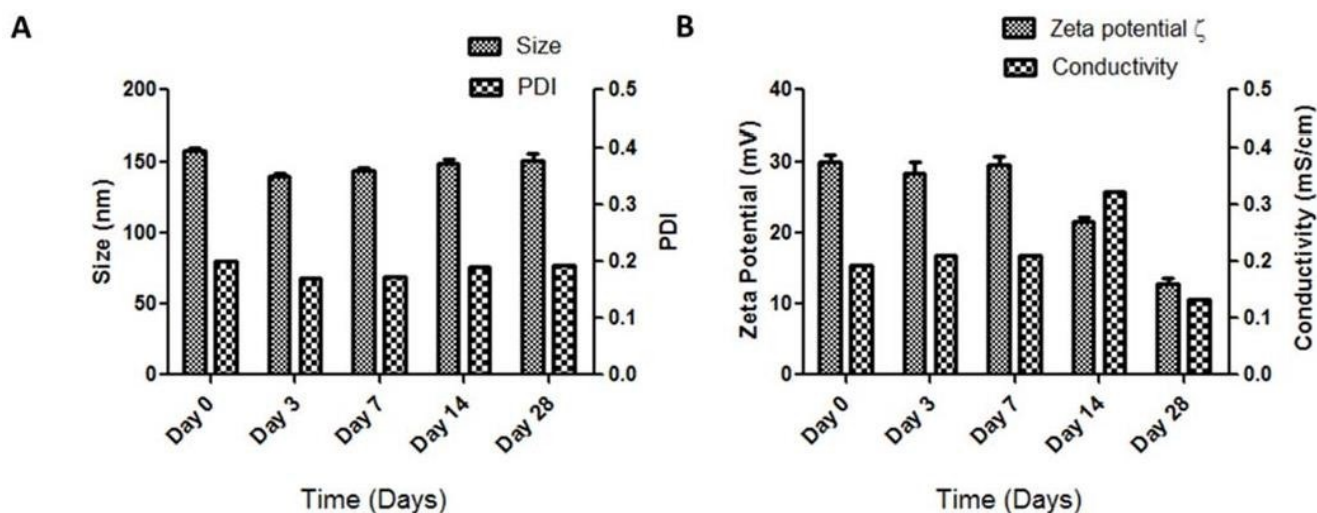


Figure 4. The graphs represent the stability study based on physicochemical parameters of the modified lipid-based nanoparticles with siRNA added before each measurement on days: 0, 3, 7, 14, and 28, indicated by (A) Size and polydispersity index (PDI) and (B) Zeta potential and conductivity values. The theoretical chitosan concentration was (1.8 mg/mL) which was the optimized chitosan concentration used for all experiments. The blank LBNP storage temperature was 4 °C.

Figures 5 and 6 show the preparation and characterisation of the siCtrl_LBNP and siCtrl_chitosan polyplex at various time periods for the second experiment. Since there was hardly any free siRNA visible in the heparin-containing circumstances, the siCtrl_LBNP could entrap siRNA for the duration of the research without experiencing any notable changes, similar to the polyplexes (Figure 5). For siCtrl_LBNP, measures of size, PDI, and zeta potential showed little variations during a 28-day period. The siRNA loading on LBNP, which makes the system more stable, is most likely the cause of this. Sizes of siCtrl_LBNP were less than 150 nm, zeta potential was around +30 mV, and PDI was less than 0.2. On the other hand, when the PDI and zeta potential values varied over time, the siCtrl_chitosan polyplexes shrank in size (Figure 6). These findings demonstrate that chitosan grafting at the LBNP surface stabilises the complex and that siCtrl_LBNPs are more stable over time than siCtrl_chitosan polyplexes. For up to 28 days,

the siRNA_LBNP formulations could be described as stable. It is important to note that we didn't go above the allotted 28 days. Fluorescent Cellular Uptake by siRNA_LBNP Confocal spectral imaging (CSI) was used to assess the cellular uptake of blank LBNP and siRNA_LBNP on SK-BR-3, a HER2+ breast cancer cell line. Instead of LAPA, the core of LBNP was encapsulated with a fluorescent dye (1,1-Dioctadecyl-3,3,3,3-tetramethylindodicarbocyanine, 4-chlorobenzenesulfonatesalt DiD), and the intracellular internalisation of siRNA and LBNP were monitored using fluorescent ATTO488-labeled siRNA, respectively. To perform the cellular uptake analysis, DiD_LBNP and ATTO488 labeled siCtrl-DiD_LBNP were characterised (Table S1). The red spectra in Figure 7A show that DiD, a lipophilic carbocyanine dye, had a maximum emission wavelength of 667 nm and manifested in the formulation as a brilliant pink colour. The size and PDI of ATTO488-labeled siRNA-DiD_LBNP were also described (Table S1). ATTO488

(green spectrum, Figure 7A) emits light with a maximum wavelength of 524 nm. After four hours of incubation with the dye-loaded LBNPs, the fluorescence signal was seen within the SK-BR-3 cells. The ATTO 488-labeled siRNA (green) was found in the perinuclear region and cytoplasm in Figure 7B. Simultaneously, the DiD_LBNP (red) was mostly located in the cytoplasm, but not exactly

precisely where (Figure 7C). Since the two fluorescences were not completely co-localized, we assumed that a successful endosomal escape of siRNA was guaranteed (Figure 7D). Our results demonstrated that the fast cellular absorption of LBNPs was unaffected by chitosan modification. The downregulation of the Survivin protein by Western blot demonstrated that the loaded siRNA could enter the cells and

evade the endosomes, enabling its RNA interference action (Figure S3). Importantly, increased cellular absorption of nanoparticles would surely aid in the therapeutic impact of the active ingredients that are loaded, increasing the medications' therapeutic effectiveness. Effective cellular uptake of LBNP was confirmed by the fluorescence signal, which mostly occurred within the cells rather than at the cell membrane.

Figure 5. Gel retardation assay images demonstrate siRNA protection of siCtrl._Chitosan in H₂O (pH < 5) and siCtrl._loaded LBNP on day 0 (A) and day 28 (B). The theoretical chitosan concentration was 1.8 mg/mL (optimized concentration). siRNA formulated in each condition in the presence (+) or absence (-) of heparin was compared to naked siRNA. Lanes without heparin show free siRNA amount, and lanes with heparin show total siRNA amount in the sample. The ctrl. siRNA was added once on day 0.

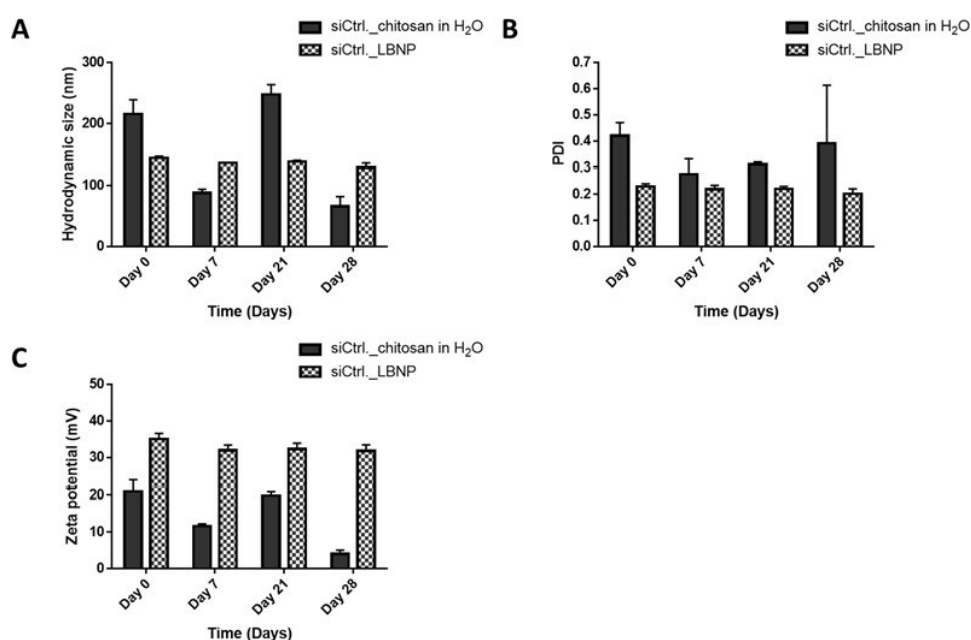


Figure 6. Stability study graphs of size (A), polydispersity index (PDI) (B), and zeta potential (C) variation over the time of siCtrl._Chitosan in H₂O (Polyplex) (pH < 5) and siCtrl._loaded LBNP. The formulation's storage temperature was 4 °C. The ctrl. siRNA was added once on day 0.

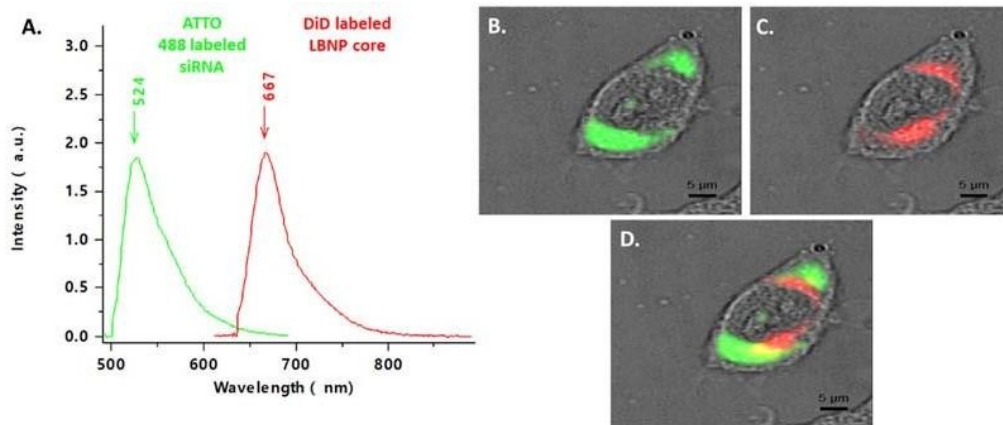


Figure 7. Uptake of fluorescent LBNP and fluorescent siRNA in SK-BR-3 cells after 4 h incubation. Cells were analyzed by confocal spectral imaging, DiI labeled LBNP are represented in red, and ATTO-488 labeled siRNA loaded LBNP in green. Representative spectra of both fluorochromes (A), representative images of each fluorochrome alone (B,C), and merged (D).

Cell Viability Analysis of LAPA_LBNP and siSurvivin-LAPA_LBNP

The cytotoxic effect of different LBNP formulations was assessed on SK-BR-3 breast cancer cells using the ATP-based cytotoxicity assay cell titer Glo[®]. As illustrated in Figure 8, the curves showed that all the formulations exhibited typical time and concentration-dependent cytotoxicity. The IC₅₀ values extracted from the cell survival curves for blank LBNP, LAPA salt, siCtrl.-LAPA_LBNP, and siSurv.-LAPA_LBNP

are presented in Table 2. Blank LBNP IC₅₀ is considered non-toxic compared to all the formulations used, as the IC₅₀ value was superior to 6 μM ($p < 0.05$) (Table 3). These results confirm that blank_LBNPs at the same range of concentration as loaded ones were not toxic to the cells, proving that the toxicity is more related to the encapsulated active contents than the carrier.

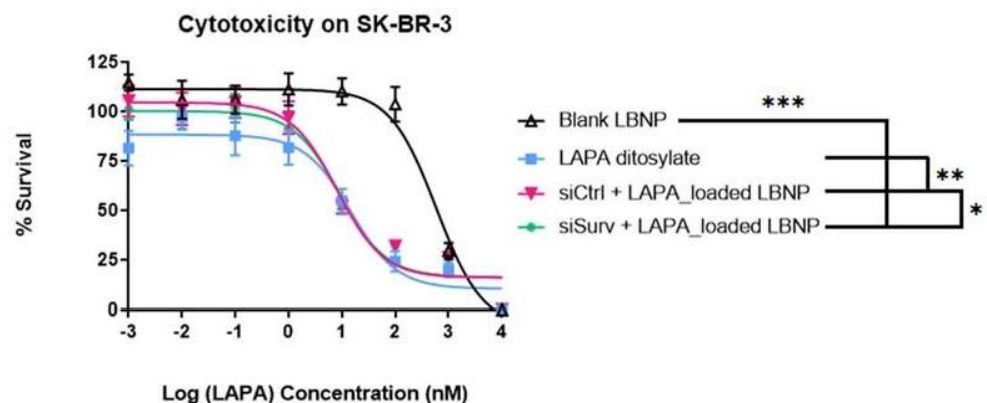


Figure 8. Dose-response curves of blank, siCtrl.-LAPA and siSurvivin-LAPA-loaded LBNP formulations; and Lapatinib dityosylate as a free drug. The half-maximal inhibitory concentration (IC₅₀) values were recalculated from cell survival curves in SK-BR-3 cells after 96 h incubation.

* p value < 0.05 (significant), ** p value < 0.01 (highly significant), *** p value < 0.001 (extremely significant).

On the other hand, the toxicity of siCtrl.-LAPA_LBNP was statistically significant compared to free LAPA ($p = 0.0006$). The IC₅₀ was around 99.7 ± 12.8 for siCtrl.-LAPA_LBNP and around 159.0 ± 12.4 for LAPA dityosylate. Higher cytotoxicity is related to more drugs transferred to cancer cells. Free drugs are available by a passive diffusion mechanism at the intracellular site. It is also worth mentioning that LAPA is a substrate of the ATP-dependent pump transporters system, mainly P-gp and ABCG2 [55,56]. It means that LAPA is pumped out of the cytoplasm before exerting its therapeutic efficacy [57]. On the contrary,

drug-loaded nanoparticles had an apparent cytotoxicity due to the nanoscale effect with a mechanism of cellular internalization by endocytosis [58]. In our case, siCtrl.-LAPA_LBNP was more efficacious than free LAPA ditosylate, which is a very interesting result. Many other drug-loaded nanoparticles reported less potent activity because the encapsulated drug needed to diffuse through the core of the nanoparticles and the

Table 2. The IC₅₀ values of different formulations of LBNP and free LAPA.

Tested Formulations	IC ₅₀ (nM)
LBNP	6481±1486
LAPA_ditosylate	159.0±12.4
siCtrl.-LAPA_LBNP	99.7±12.8
siSurv.-LAPA_LBNP	76.8±12.3

LBNP: Lipid-based nanoparticles, LAPA: Lapatinib, siCtrl.: Control siRNA, siSurv.: anti-Survivin siRNA, IC₅₀: Half-maximal inhibitory concentration.

Table 3. Actual *p* values of control and tested formulations calculated based on IC₅₀ variations obtained from the cytotoxicity assay.

Formulations	Statistical Significance	Control	Evaluated/Compared	<i>p</i> -Value
siCtrl.-LAPA_LBNP				
LBNP			siSurv.-LAPA_LBNP Ditosylate	LAPA 0.0001***
siCtrl.-LAPA_LBNP		LAPA Ditosylate		0.0006***
siCtrl.-LAPA_LBNP		siSurv.-LAPA_LBNP		0.0418*

LBNP: Lipid-based nanoparticles, LAPA: Lapatinib, siCtrl.: Control siRNA, siSurv.: anti-Survivin siRNA.
 p*value < 0.05 (significant), **p*value < 0.001 (extremely significant).

In addition, siSurvivin-LAPA_LBNP showed a more substantial effect on decreasing cell viability compared to siCtrl.-LAPA_LBNP, indicating that anti-Survivin siRNA and LAPA had synergistic anti-cancer effects (Figure 8 and Table 3). However, this synergy was marginal (*p*= 0.0418), meaning that further optimization must be carried out to achieve the maximal effect of the combination. The superior cytotoxic effect of siSurvivin-LAPA_LBNP was attributed to the additive effect of the downregulation of Survivin due to siRNA and LAPA co-vectorization. Xia et al. studied the relationship between Survivin protein downregulation and Lapatinib usage in HER2 overexpressing tumors. They concluded that selective knockdown of HER2 using small interfering RNA markedly reduced Survivin protein, resulting in apoptosis of HER2-overexpressing breast cancer cell lines such as BT-474. Alternatively, at relevant concentrations, inhibition of ErbB2 signaling using Lapatinib, a reversible HER2/EGFR tyrosine kinase inhibitor, leads to marked inhibition of Survivin protein resulting in cell apoptosis. The effect of Lapatinib on Survivin seems to be predominantly post-translational [60]. If the knockdown of the Survivin protein plays a role in lapatinib-induced apoptosis, then Survivin overexpression might protect cells from the therapeutic action of Lapatinib. Moreover, if the regulation of Survivin by Lapatinib is solely transcriptionally mediated, then

reach the cytoplasm compartment, while the free drug is easily accessible to their sites of action [59]. Although Lapatinib had a dual inhibition of HER2 and EGFR against overexpressed HER2 breast cancer, the drug cannot completely inhibit cell proliferation in the eHER2+ cell line model. We conclude that the siCtrl.-LAPA_LBNP had a better effect than the Lapatinib salt, which provides an excellent alternative parenteral dosage form of Lapatinib.

Lapatinib would not be expected to reduce His-tagged Survivin protein, which is under the transcription of another promoter. Their finding provides a rationale for combining Lapatinib with small interfering RNA regulating apoptosis, leading to apparent cell death [60].

2. Materials and Methods

Materials

Tetrahydrofuran (THF), sodium chloride, and anhydrous dimethyl sulfoxide (DMSO) were acquired from Carlo Erba Reagents (Normandie, France). Sigma Aldrich (Saint-Quentin-Fallavier, France) supplied the glycine. BASF (Ludwigshafen, Germany) provided the macrogol glycerides and Kolliphor HS15® (Macrogol 15- Hydroxystearate) and Labrafac®WL 1349 (triglyceride containing 50–80% caprylic acid and 20–50% capric acid). Gattefosse S.A. (Saint-Priest, France) generously supplied Labrasol® (30% mono-, di-, and triglycerides of C8 and C10 fatty acids, 50% mono- and diesters of PEG, and 20% of free PEG 400). Acros Organic (France) supplied lapatinib (Mw = 581.1 g/mol), whereas Lipoid (Lipoid GmbH, Ludwigshafen, Germany) supplied Lipoid®S75-3. Invitrogen™ (Waltham, MA, USA) supplied the DiD fluorescent dye (1,10-dioctadecyl-3,3',3,3'-tetramethylindodicarbocyanine, 4-chlorobenzenesulfonate salt). From Sigma–Aldrich Chemie GmbH (Schnelldorf, Germany), chitosan oligosaccharide lactate (MW 5000; degree of acetylation: ≤90%) was acquired. BioValley (Marne La Vallée, France) supplied the dialysis membranes (molecular weight cut-off (MWCO) 100 kDa, regenerated cellulose). Promega (Madison, WI, USA) provided the cell titer Glo® kit. Model siRNA (sense sequence 5'-3' GGAAGAUCAUAAUGGACAGdTdT with lowercase letters denoting deoxyribonucleotides) was acquired from Eurogentec (Angers, France) either unlabelled or labelled with ATTO488 (at the "5' position of the sense strand). Sigma Aldrich Chemie GmbH (St. Quentin Fallavier, France) supplied the siRNA against Survivin, which contains the sense sequence 5'-3' GUCUGGACCUCAUGUUGUdTdT, where the lowercase letters stand for deoxyribonucleotides. Agarose, ethidium bromide, and loading buffer for gel retardation tests were purchased from Fisher Bioreagents® (Illkirch, France). Life Technologies (Paisley, UK) provided all of the culture-related media and supplements. A Milli-Q system (Millipore, Paris, France) provided the water.

Nanocarrier Preparation

Formulation of LAPA-Loaded Lipid Nanocapsules

With minor adjustments, LAPA-loaded lipid nanocapsules (LAPA_LNCs) were made using the phase inversion temperature approach as outlined by Malzert-Fréon et al. [25]. The active was encased in the centre of the nanoparticles, which included a combination of the lipophilic vehicle solubilizer Labrafac®WL 1349 and the solubility enhancer Labrasol®. To guarantee full drug dissolution, Lapatinib (0.35–0.63% w/w) was first dissolved in Labrasol® (10.24–10.51% w/w) while being continuously shaken and heated to a temperature lower than the drug's melting point (136–150 °C). Next, water (21.73% w/w), Labrafac®WL 1349 (4.3% w/w), Kolliphor®HS15 (7.59% w/w), Lipoid®S75-3 (0.673% w/w), and NaCl (0.87% w/w) were added, and the mixture was heated to 85 °C while being stirred magnetically. Between 85°C and 45°C, three progressive heating and cooling cycles were conducted. The mixture was supplemented with 2 °C deionised water (53.89% w/w) during the inversion phase (61–63 °C) of the final cooling cycle. To create LAPA_LNCs, the formulation was then combined for an additional five

minutes while being stirred magnetically. To track the subsequent cell absorption, fluorophore-loaded lipid nanocapsules (DiD_LNCs) were created. To manufacture DiD_LNCs, the dye was dissolved in 2% of the core using both Labrasol® (10.68% w/w) and Labrafac®WL1349 (4.35% w/w) until the dye was completely dissolved. The remainder of the procedure didn't change. As control formulations, blank LNCs loaded with no active ingredients were used. Labrasol® (10.87% w/w) and Labrafac®WL 1349 (4.35% w/w) were combined directly with the other ingredients for blank LNCs, and the heating-cooling cycles were carried out as previously mentioned. creation of co-loaded siRNA Nanoparticles Based on Lipids To generate LBNP, a transacylation process between the functional amino group of the chitosan oligosaccharide lactate polymer and the pegylated hydroxy stearate was conducted. It was an adaptation of a technique previously reported by Messaoudi et al. [33]. In short, 20 millilitres of blank LNCs, LAPA LNCs, or DiD LNCs were combined with one millilitre of NaOH 10M and three distinct concentrations of chitosan (0.6, 1.2, and 1.8 mg/mL), which are referred to as schitosan 1×, 2×, and 3×, respectively. After 15 minutes in a 25°C water bath, the reaction was halted by adding 20 mL of glycine buffer. Lastly, a dialysis-based purification step using membranes with a 100 KDa molecular weight cut-off was carried out for 24 hours using Milli-Q water while being stirred magnetically. For the first three hours, water was changed every hour. As the free unbound chitosan dispersed in the dialysis water, transacylated nanoparticles—henceforth referred to as lipid-based nanoparticles, or LBNP—were able to stay within the dialysis membrane. In order to properly ionise the chitosan prior to the electrostatic addition of the siRNA, the final LBNP was then adjusted to 1-2 using an HCl solution. The LBNP suspension was then vortexed for 10 seconds after the siRNA solution was added at a volume ratio of 1:3. The siRNA_LBNP, siRNA-LAPA_LBNP, or siRNA-DiD_LBNP that were produced were employed right away for either additional cellular investigations or for nanocarrier characterisation. The siRNA solution's concentration was modified based on its intended purpose. Nanocarrier Particle Size and Zeta Potential Physicochemical Features The Malvern NanoZS instrument (Malvern Instruments, Malvern, UK) was used to assess the formulation's size, polydispersity index, and zeta potential. After diluting the (blank or loaded) LNCs and LBNPs suspension by a factor of 10 and 60, respectively, in Milli-Q water at 25°C, the size measurement was carried out. The conductivity values for zeta potentials were similar across all formulations. Every measurement was carried out three times. Efficiency of Encapsulation

To confirm that the various formulation procedures did not impair LAPA_LBNP integrity, the quantity of LAPA encapsulated in LNCs was measured immediately after LAPA_LNCs formulation, LAPA_LBNP purification, and pH adjustment to pH 1-2. To remove free LAPA from LNCs/LBNB solution, each batch was filtered using a polyether sulfone® 0.2 µm filter (Clearline, D. Dutscher, Brumath, France). Filtrated and non-filtrated samples of each batch were made by dissolving 125 µL of LAPA-loaded LNCs/LBNP in an equal amount of water and THF (1 mL). The absorbance of the solution was then measured between 250 and 400 nm using a UV-visible spectrophotometer (Genesys 10S, ThermoScientific, France). By comparing the LAPA absorbance at 335 nm to a

calibration curve created using blank nanocarriers and an LAPA/THF/water combination, quantification was accomplished. The following formulae were used to compute drug loading (DL = quantity of LAPA per weight of LNCs suspension; mg/g) and encapsulation efficiency (EE) (%). The LAPA concentration in the LNCs suspension ($M_w = 581.1$ g/mol) was also given in molarity, where the density of the LNCs suspension is equivalent to that of water. Weight of LAPA in LNCs suspension (mg)/weight of LNCs (g) = DL(mg/g) Encapsulated Lapatinib/Total Lapatinib $\times 100$ = EE (%) Gel Electrophoresis of Agarose

To verify the complexation of siRNA into the nanocarrier, an agarose gel electrophoresis experiment was used. In order to achieve a final siRNA concentration of 1.2 μ M per well, samples were produced. Samples were utilised both with and without heparin (final concentration of 3 mg/mL) to maintain the integrity of the formulations and release siRNA (Sigma-

Germany's Steinheim is home to Aldrich Chemie GmbH. Before the samples were loaded into the wells, a loading buffer (2X RNA loading dye, Life Technologies, Paisley, United Kingdom) was added. Agarose (Low-EEO/Multi-Purpose, Acros Organics BV, Gel, Belgium) was dissolved in Tris-acetate-EDTA (TAE) solution 1X (Acros Organics BV, Gel, Belgium) containing 0.01% (v/v) ethidium bromide (EtBr) to visualise free siRNA to create an agarose gel (1% m/v). Following sample deposition on the agarose gel, electrophoresis migration was carried out for 15 minutes at 150V in TAE 1X buffer. The gels were visualised by UV imaging on a Fusion-Solo.65.WL imager (Vilbert Lourmat, Marne-la-Vallée, France) using the EvolutionCapt software. The stability of the nanoparticles' storage Initially, blank LBNPs were kept at a low temperature (4 °C) and shielded from light. They had three distinct chitosan concentrations (1 \times , 2 \times , and 3 \times , respectively). Following the siRNA addition, measurements were made of the particle size, PDI, and zeta potential on days 0, 7, 14, 21, and 28. After that, gel agarose electrophoresis was used to conduct a siRNA complexation experiment. The purpose of these tests was to examine the stability of blank LBNPs, as well as their capacity to maintain their physicochemical properties and siRNA loading over time. Additional details on the comparison of the three formulations are included in the Supplementary Information (Figure S1). Using siRNA_LBNP and free siRNA-chitosan made by physically mixing with water, the storage stability of optimised LBNP with a 3 \times chitosan concentration (1.8 mg/mL) was examined. In this instance, the RNA was introduced on day 0 and monitored throughout time. For up to 28 days at 4 °C, all of the formulations were stored as previously described, and on days 0, 7, 14, and 28, they were all described in the same manner. Evaluation of Nanocarrier Cellular Culture and Cell Line Cell Lines Service (CLS Eppelheim, Germany) provided the SK-BR-3 human breast cancer cell lines with HER2 overexpression. Dulbecco's Modified Eagle Medium (DMEM) supplemented with 10% foetal bovine serum (FBS, Gibco®) and 1% Penicillin-Streptomycin solution (10,000 U/mL, Gibco®) was used to cultivate SK-BR-3 cells at 37 °C and 5% CO₂. CSI, or Confocal Spectral Imaging The distribution of ATTO488 siRNA-DiD_LBNP on cell-adherent coverslips was examined for confocal spectral

imaging. 24-well plates were filled with cover glasses that had been coated with poly-D-lysine. After being seeded with 3 $\times 10^4$ SK-BR-3 cells, they were left in a growth medium for 48 hours. After that, the cells were treated with ATTO488-labeled siRNA-DiD_LBNP (final siRNA concentration of 150 nM) in OptiMEM for four hand washings with PBS. A LabRAM laser scanning confocal microspectrometer (Horiba SA, Villeneuve d'Ascq, France) with a 300/mm diffraction grating and a CCD detector air-cooled by Peltier effect was used to scan the cover glasses for CSI. The glasses were positioned between a microscope slide and a coverslip. A built-in He-Ne laser's 633 nm line was used to excite the DiD fluorescence, and a 491 nm laser was used to excite the ATTO488 fluorescence under a 50X long focal microscope lens. The collection duration was 50 ms per spectra, and the laser light output at the sample was around 0.1 mW. An optical section (x-y plane) at half the cell thickness was scanned at a step of 0.8 μ m to analyse adherent cells. The resulting maps generally included 2500 spectra. Using LabSpec software version 5, multispectral maps were acquired and processed. In Vitro

Cytotoxicity

A luminous test based on the measurement of ATP utilising the Cell Titer-Glo cell Proliferation Assay (Promega, Madison, WI, USA) was used to examine cell viability and proliferation. In short, 100 μ L of the medium was used to incubate 6000 SK-BR-3 cells in 96 well plates.

plates for 24 hours, after which they were exposed to doses of the tested chemicals ranging from 0.01 nM to 100 μ M. The culture medium by itself was evaluated as a negative control, while a 20 mM H₂O₂ solution served as a positive control. Cells were examined with LAPA ditosylate salt, LBNP loaded with either Ctrl.siRNA or anti-Survivins siRNA, and blank LBNP. For four days, 100 μ L of each solution was incubated with cells at 37 °C with 5% CO₂. Then, the Cell Titer-Glo agent (Promega, Madison, WI, USA) was used to evaluate cell viability. In short, each well received 100 μ L of Cell Titer-Glo agent after 100 μ L of Themiemium was withdrawn. After two minutes of shaking, the plates were incubated for ten minutes at room temperature. The absorbance microplate reader (Bio-Tek® instruments, Inc., Winooski, VT, USA) was used to measure the luminescence values with an acquisition at 0.5s. Graphpad PRISM 7 software was used to determine the 50% inhibitory concentration (IC₅₀) when dose-dependent activity was detected (n = 4 in quadruplicate). Analytical Statistics

Every formulation was made at least three times for physicochemical characterisation. The mean \pm standard deviation is used to display all data. GraphPad PRISM 7 software was used to determine the IC₅₀ and p values.

3. Conclusions

In conclusion, the present work examined the possibility of a synergistic therapeutic impact on the HER2-overexpressed SK-BR-3 cell line by the co-delivery of LAPA and anti-Survivin siRNA in modified lipid nanocapsules. As a parenteral administration method, the siSurvivin-LAPA_LBNP demonstrated appropriate physicochemical characteristics. The combination significantly reduces the expression of the Survivin protein, causes cell death, and effectively suppresses cell growth. The beneficial anti-cancer impact was ascribed to the combined action of LAPA's effectiveness and the in vitro maintenance of apoptotic

induction by Survivin protein knockdown. Despite the fact that this synergy was not as strong as anticipated, our results add credence to the mounting evidence that siRNA therapy in conjunction with anti-cancer medications offers a novel therapeutic approach for HER2+, one of the most aggressive forms of breast cancer. In the future, an in vivo model with many protein targets involved in controlling genes responsible for MDR, apoptosis, and other cancer cell survival pathways might be used to further validate and evaluate this novel treatment.

References

- Sung, H.; Ferlay, J.; Siegel, R.L.; Laversanne, M.; Soerjomataram, I.; Jemal, A.; Bray, F. Global Cancer Statistics 2020: GLOBOCAN Estimates of Incidence and Mortality Worldwide for 36 Cancers in 185 Countries. *CA Cancer J. Clin.* **2021**, *71*, 209–249. [[CrossRef](#)]
- Nuciforo, P.; Radosevic-Robin, N.; Ng, T.; Scaltriti, M. Quantification of HER Family Receptors in Breast Cancer. *Breast Cancer Res.* **2015**, *17*, 53. [[CrossRef](#)]
- Schlam, J.; Swain, S.M. HER2-Positive Breast Cancer and Tyrosine Kinase Inhibitors: The Time Is Now. *Npj Breast Cancer* **2021**, *7*, 56. [[CrossRef](#)] [[PubMed](#)]
- Costa, R.L.B.; Czerniecki, B.J. Clinical Development of Immunotherapies for HER2+ Breast Cancer: A Review of HER2-Directed Monoclonal Antibodies and Beyond. *Npj Breast Cancer* **2020**, *6*, 10. [[CrossRef](#)] [[PubMed](#)]
- Slamon, D.J.; Leyland-Jones, B.; Shak, S.; Fuchs, H.; Paton, V.; Bajamonde, A.; Fleming, T.; Eiermann, W.; Wolter, J.; Pegram, M.; et al. Use of Chemotherapy plus a Monoclonal Antibody against HER2 for Metastatic Breast Cancer That Overexpresses HER2. *N. Engl. J. Med.* **2001**, *344*, 783–792. [[CrossRef](#)]
- Slamon, D.; Eiermann, W.; Robert, N.; Pienkowski, T.; Martin, M.; Press, M.; Mackey, J.; Glaspy, J.; Chan, A.; Pawlicki, M.; et al. Adjuvant Trastuzumab in HER2-Positive Breast Cancer. *N. Engl. J. Med.* **2011**, *365*, 1273–1283. [[CrossRef](#)] [[PubMed](#)]
- Ferraro, E.; Drago, J.Z.; Modi, S. Implementing Antibody-Drug Conjugates (ADCs) in HER2-Positive Breast Cancer: State of the Art and Future Directions. *Breast Cancer Res.* **2021**, *23*, 84. [[CrossRef](#)] [[PubMed](#)]
- Dai, C.; Tiwari, A.K.; Wu, C.-P.; Su, X.; Wang, S.-R.; Liu, D.; Ashby, C.R.; Huang, Y.; Robey, R.W.; Liang, Y.; et al. Lapatinib (Tykerb, GW572016) Reverses Multidrug Resistance in Cancer Cells by Inhibiting the Activity of ATP-Binding Cassette Subfamily B Member 1 and G Member 2. *Cancer Res.* **2008**, *68*, 7905–7914. [[CrossRef](#)]
- Ratain, M.J.; Cohen, E.E. The Value Meal: How to Save \$1,700 Per Month or More on Lapatinib. *J. Clin. Oncol.* **2007**, *25*, 3397–3398. [[CrossRef](#)]
- Tsang, R.Y.; Sadeghi, S.; Finn, R.S. Lapatinib, a Dual-Targeted Small Molecule Inhibitor of EGFR and HER2, in HER2-Amplified Breast Cancer: From Bench to Bedside. *Clin. Med. Insights Ther.* **2011**, *3*, CMT.S3783. [[CrossRef](#)]
- Gao, H.; Wang, Y.; Chen, C.; Chen, J.; Wei, Y.; Cao, S.; Jiang, X. Incorporation of Lapatinib into Core-Shell Nanoparticles Improves Both the Solubility and Anti-Glioma Effect of the Drug. *Int. J. Pharm.* **2014**, *461*, 478–488. [[CrossRef](#)] [[PubMed](#)]
- Medina, P.; Goodin, S. Lapatinib: A Dual Inhibitor of Human Epidermal Growth Factor Receptor Tyrosine Kinases. *Clin. Ther.* **2008**, *30*, 1426–1447. [[CrossRef](#)] [[PubMed](#)]
- Eljack, S.; David, S.; Faggad, A.; Chourpa, I.; Allard-Vannier, E. Nanoparticles Design Consideration to Co-Deliver Nucleic Acids and Anti-Cancer Drugs for Chemoresistance Reversal. *Int. J. Pharm. X* **2022**, *4*, 100126. [[CrossRef](#)]
- Greco, F.; Vicent, M.J. Combination Therapy: Opportunities and Challenges for Polymer-Drug Conjugates as Anticancer Nanomedicines. *Adv. Drug Deliv. Rev.* **2009**, *61*, 1203–1213. [[CrossRef](#)]
- Tanizaki, J.; Okamoto, I.; Fumita, S.; Okamoto, W.; Nishio, K.; Nakagawa, K. Roles of BIM Induction and Survivin Downregulation in Lapatinib-Induced Apoptosis in Breast Cancer Cells with HER2 Amplification. *Oncogene* **2011**, *30*, 4097–4106. [[CrossRef](#)] [[PubMed](#)]
- Altieri, D.C. Survivin, Versatile Modulation of Cell Division and Apoptosis in Cancer. *Oncogene* **2003**, *22*, 8581–8589. [[CrossRef](#)]
- Altieri, D.C. Validating Survivin as a Cancer Therapeutic Target. *Nat. Rev. Cancer* **2003**, *3*, 46–54. [[CrossRef](#)] [[PubMed](#)]
- Ambrosini, G.; Adida, C.; Altieri, D.C. A Novel Anti-Apoptosis Gene, Survivin, Expressed in Cancer and Lymphoma. *Nat. Med.* **1997**, *3*, 917–921. [[CrossRef](#)]
- Li, F.; Ambrosini, G.; Chu, E.Y.; Plescia, J.; Tognin, S.; Marchisio, P.C.; Altieri, D.C. Control of Apoptosis and Mitotic Spindle Checkpoint by Survivin. *Nature* **1998**, *396*, 580–584. [[CrossRef](#)]
- Sun, W.; Chen, X.; Xie, C.; Wang, Y.; Lin, L.; Zhu, K.; Shuai, X. Co-Delivery of Doxorubicin and Anti-BCL-2 siRNA by PH-Responsive Polymeric Vector to Overcome Drug Resistance in In Vitro and In Vivo HepG2 Hepatoma Model. *Biomacromolecules* **2018**, *19*, 2248–2256. [[CrossRef](#)]
- Majumder, J.; Minko, T. Multifunctional Lipid-Based Nanoparticles for Co-Delivery of Anticancer Drugs and siRNA for Treatment of Non-Small Cell Lung Cancer with Different Level of Resistance and EGFR Mutations. *Pharmaceutics* **2021**, *13*, 1063. [[CrossRef](#)]
- Babaei, M.; Abnous, K.; Taghdisi, S.M.; Taghavi, S.; Saljooghi, A.S.; Ramezani, M.; Alibolandi, M. Targeted Rod-Shaped Mesoporous Silica Nanoparticles for the Co-Delivery of Camptothecin and Survivin shRNA in to Colon Adenocarcinoma In Vitro and In Vivo. *Eur. J. Pharm. Biopharm.* **2020**, *156*, 84–96.

- [CrossRef]
23. Heurtault, B.; Saulnier, P.; Pech, B.; Proust, J.; Benoit, J. A Novel Phase Inversion-Based Process for the Preparation of Lipid Nanocarriers. *Pharm. Res.* **2002**, *19*, 875–880. [CrossRef]
 24. Allard, E.; Passirani, C.; Garcion, E.; Pigeon, P.; Vessières, A.; Jaouen, G.; Benoit, J.-P. Lipid Nanocapsules Loaded with an Organometallic Tamoxifen Derivative as a Novel Drug-Carrier System for Experimental Malignant Gliomas. *J. Control. Release* **2008**, *130*, 146–153. [CrossRef]
 25. Malzert-Fréon, A.; Saint-Lorant, G.; Hennequin, D.; Gauduchon, P.; Poulain, L.; Rault, S. Influence of the Introduction of a Solubility Enhancer on the Formulation of Lipidic Nanoparticles with Improved Drug Loading Rates. *Eur. J. Pharm. Biopharm.* **2010**, *75*, 117–127. [CrossRef]
 26. David, S.; Resnier, P.; Guillot, A.; Pitard, B.; Benoit, J.-P.; Passirani, C. SiRNA LNCs—A Novel Platform of Lipid Nanocapsules for Systemic SiRNA Administration. *Eur. J. Pharm. Biopharm.* **2012**, *81*, 448–452. [CrossRef][PubMed]
 27. Resnier, P.; Galopin, N.; Sibiril, Y.; Clavreul, A.; Cayon, J.; Briganti, A.; Legras, P.; Vessières, A.; Montier, T.; Jaouen, G.; et al. Efficient Ferrocifen Anticancer Drug and Bcl-2 Gene Therapy Using Lipid Nanocapsules on Human Melanoma Xenograft in Mouse. *Pharmacol. Res.* **2017**, *126*, 54–65. [CrossRef]
 28. Resnier, P.; Lepeltier, E.; Emina, A.L.; Galopin, N.; Bejaud, J.; David, S.; Ballet, C.; Benvegno, T.; Pecorari, F.; Chourpa, I.; et al. Model Affitin and PEG Modifications onto SiRNA Lipid Nanocapsules: Cell Uptake and *in Vivo* Biodistribution Improvements. *RSC Adv.* **2019**, *9*, 27264–27278. [CrossRef]
 29. Bastiancich, C.; Bozzato, E.; Luyten, U.; Danhier, F.; Bastiat, G.; Prétat, V. Drug Combination Using an Injectable Nanomedicine Hydrogel for Glioblastoma Treatment. *Int. J. Pharm.* **2019**, *559*, 220–227. [CrossRef][PubMed]
 30. Labrak, Y.; Heurtault, B.; Frisch, B.; Saulnier, P.; Lepeltier, E.; Miron, V.E.; Muccioli, G.G.; des Rieux, A. Impact of Anti-PDGFR α Antibody Surface Functionalization on LNC Uptake by Oligodendrocyte Progenitor Cells. *Int. J. Pharm.* **2022**, *618*, 121623. [CrossRef][PubMed]
 31. Lollo, G.; Matha, K.; Bocchiardo, M.; Bejaud, J.; Marigo, I.; Virgone-Carlotta, A.; Dehoux, T.; Rivière, C.; Rieu, J.-P.; Briançon, S.; et al. Drug Delivery to Tumours Using a Novel 5-FU Derivative Encapsulated into Lipid Nanocapsules. *J. Drug Target.* **2019**, *27*, 634–645. [CrossRef][PubMed]
 32. Levy, M.-C.; Edwards-Levy, F. Coating Alginate Beads with Cross-Linked Biopolymers: A Novel Method Based on a Transacylation Reaction. *J. Microencapsul.* **1996**, *13*, 169–183. [CrossRef][PubMed]
 33. Messaoudi, K.; Saulnier, P.; Boesen, K.; Benoit, J.-P.; Lagarce, F. Anti-Epidermal Growth Factor Receptor SiRNA Carried by Chitosan-Transacylated Lipid Nanocapsules Increases Sensitivity of Glioblastoma Cells to Temozolomide. *Int. J. Nanomed.* **2014**, *9*, 1479. [CrossRef]
 34. Djekic, L.; Primorac, M. The Influence of Cosurfactant and Oil on the Formation of Pharmaceutical Microemulsions Based on PEG-8 Caprylic/Capric Glycerides. *Int. J. Pharm.* **2008**, *352*, 231–239. [CrossRef][PubMed]
 35. Hu, Z.; Tawa, R.; Konishi, T.; Shibata, N.; Takada, K. A Novel Emulsifier, Labrasol, Enhances Gastrointestinal Absorption of Gentamicin. *Life Sci.* **2001**, *69*, 2899–2910. [CrossRef][PubMed]
 36. Libster, D.; Aserin, A.; Wachtel, E.; Shoham, G.; Garti, N. An HILIC Liquid Crystal-Based Delivery System for Cyclosporin A: Physical Characterization. *J. Colloid Interface Sci.* **2007**, *308*, 514–524. [CrossRef]
 37. Katas, H.; Alpar, H.O. Development and Characterisation of Chitosan Nanoparticles for SiRNA Delivery. *J. Control. Release* **2006**, *115*, 216–225. [CrossRef]
 38. Li, J.; Cai, C.; Li, J.; Li, J.; Sun, T.; Wang, L.; Wu, H.; Yu, G. Chitosan-Based Nanomaterials for Drug Delivery. *Molecules* **2018**, *23*, 2661. [CrossRef]
 39. Jadidi-Niaragh, F.; Atyabi, F.; Rastegari, A.; Kheshtchin, N.; Arab, S.; Hassannia, H.; Ajami, M.; Mirsanei, Z.; Habibi, S.; Masoumi, F.; et al. CD73 Specific SiRNA Loaded Chitosan Lactate Nanoparticles Potentiate the Antitumor Effect of a Dendritic Cell Vaccine in 4T1 Breast Cancer Bearing Mice. *J. Control. Release* **2017**, *246*, 46–59. [CrossRef]
 40. Benchamas, G.; Huang, G.; Huang, S.; Huang, H. Preparation and Biological Activities of Chitosan Oligosaccharides. *Trends Food Sci. Technol.* **2021**, *107*, 38–44. [CrossRef]
 41. Abrica-González, P.; Zamora-Justo, J.A.; Sotelo-López, A.; Vázquez-Martínez, G.R.; Balderas-López, J.A.; Muñoz-Diosdado, A.; Ibáñez-Hernández, M. Gold Nanoparticles with Chitosan, N-Acetylated Chitosan, and Chitosan Oligosaccharides as DNA Carriers. *Nanoscale Res. Lett.* **2019**, *14*, 258. [CrossRef][PubMed]
 42. Bellich, B.; D'Agostino, I.; Semeraro, S.; Gamini, A.; Cesàro, A. “The Good, the Bad and the Ugly” of Chitosans. *Mar. Drugs* **2016**, *14*, 99. [CrossRef][PubMed]
 43. Mohammed, M.; Syeda, J.; Wasan, K.; Wasan, E. An Overview of Chitosan Nanoparticles and Its Application in Non-Parenteral Drug Delivery. *Pharmaceutics* **2017**, *9*, 53. [CrossRef]
 44. Zargar, V.; Asghari, M.; Dashti, A. A Review on Chitin and Chitosan Polymers: Structure, Chemistry, Solubility, Derivatives, and Applications. *Chem Bio Eng Rev.* **2015**, *2*, 204–226. [CrossRef]
 45. Buss, J.H.; Begnini, K.R.; Bruinsmann, F.A.; Ceolin, T.; Sonogo, M.S.; Pohlmann, A.R.; Guterres, S.S.; Collares, T.; Seixas, F.K. Lapatinib-Loaded Nanocapsules Enhance Antitumoral Effect in Human Bladder Cancer Cell. *Front. Oncol.* **2019**, *9*, 203. [CrossRef]

46. Wilson, J.N.; Liu, W.; Brown, A.S.; Landgraf, R. Binding-Induced, Turn-on Fluorescence of the EGFR/ERBB Kinase Inhibitor, Lapatinib. *Org. Biomol. Chem.* **2015**, *13*, 5006–5011. [[CrossRef](#)] [[PubMed](#)]
47. Arvizo, R.R.; Miranda, O.R.; Thompson, M.A.; Pabelick, C.M.; Bhattacharya, R.; Robertson, J.D.; Rotello, V.M.; Prakash, Y.S.; Mukherjee, P. Effect of Nanoparticle Surface Charge at the Plasma Membrane and Beyond. *Nano Lett.* **2010**, *10*, 2543–2548. [[CrossRef](#)] [[PubMed](#)]
48. Carlson, C.; Hussain, S.M.; Schrand, A.M.; Braydich-Stolle, L.K.; Hess, K.L.; Jones, R.L.; Schlager, J.J. Unique Cellular Interaction of Silver Nanoparticles: Size-Dependent Generation of Reactive Oxygen Species. *J. Phys. Chem. B* **2008**, *112*, 13608–13619. [[CrossRef](#)]
49. Jiang, J.; Oberdörster, G.; Elder, A.; Gelein, R.; Mercer, P.; Biswas, P. Does Nanoparticle Activity Depend upon Size and Crystal Phase? *Nanotoxicology* **2008**, *2*, 33–42. [[CrossRef](#)]
50. Thorek, D.L.J.; Tsourkas, A. Size, Charge and Concentration Dependent Uptake of Iron Oxide Particles by Non-Phagocytic Cells. *Biomaterials* **2008**, *29*, 3583–3590. [[CrossRef](#)]
51. Chenthamara, D.; Subramaniam, S.; Ramakrishnan, S. G.; Krishnaswamy, S.; Essa, M.M.; Lin, F.-H.; Qoronfle, M.W. Therapeutic Efficacy of Nanoparticles and Routes of Administration. *Biomater. Res.* **2019**, *23*, 20. [[CrossRef](#)] [[PubMed](#)]
52. Phan, H.T.; Haes, A.J. What Does Nanoparticle Stability Mean? *J. Phys. Chem. C* **2019**, *123*, 16495–16507. [[CrossRef](#)] [[PubMed](#)]
53. Vecer, M.; Pospíšil, J. Stability and Rheology of Aqueous Suspensions. *Procedia Eng.* **2012**, *42*, 1720–1725. [[CrossRef](#)]
54. Mouzouvi, C.R.A.; Umerska, A.; Bigot, A.K.; Saulnier, P. Surface Active Properties of Lipid Nanocapsules. *PLoS ONE* **2017**, *12*, e0179211. [[CrossRef](#)]
55. Dunne, G.; Breen, L.; Collins, D.M.; Roche, S.; Clynes, M.; O'Connor, R. Modulation of P-Gp Expression by Lapatinib. *Investig. New Drugs* **2011**, *29*, 1284–1293. [[CrossRef](#)]
56. Polli, J.W.; Olson, K.L.; Chism, J.P.; St John-Williams, L.; Yeager, R.L.; Woodard, S.M.; Otto, V.; Castellino, S.; Demby, V.E. An Unexpected Synergist Role of P-Glycoprotein and Breast Cancer Resistance Protein on the Central Nervous System Penetration of the Tyrosine Kinase Inhibitor Lapatinib (*N*-{3-Chloro-4-[(3-Fluorobenzyl)Oxy]Phenyl}-6-[5-({2-(Methylsulfonyl)Ethyl}Amino)methyl]-2-Furyl]-4-Quinazolinamine; GW572016): TABLE 1. *Drug Metab. Dispos.* **2009**, *37*, 439–442. [[CrossRef](#)] [[PubMed](#)]
57. Ramirez, M.; Rajaram, S.; Steininger, R.J.; Osipchuk, D.; Roth, M.A.; Morinishi, L.S.; Evans, L.; Ji, W.; Hsu, C.-H.; Thurley, K.; et al. Diverse Drug-Resistance Mechanisms Can Emerge from Drug-Tolerant Cancer Persister Cells. *Nat. Commun.* **2016**, *7*, 10690. [[CrossRef](#)] [[PubMed](#)]
58. Cheng, R.; Meng, F.; Deng, C.; Klok, H.-A.; Zhong, Z. Dual and Multi-Stimuli Responsive Polymeric Nanoparticles for Programmed Site-Specific Drug Delivery. *Biomaterials* **2013**, *34*, 3647–3657. [[CrossRef](#)]
59. Yamashita, F.; Hashida, M. Pharmacokinetic Considerations for Targeted Drug Delivery. *Adv. Drug Deliv. Rev.* **2013**, *65*, 139–147. [[CrossRef](#)]
60. Xia, W.; Bisi, J.; Strum, J.; Liu, L.; Carrick, K.; Graham, K.M.; Treece, A.L.; Hardwicke, M.A.; Dush, M.; Liao, Q.; et al. Regulation of Survivin by ErbB2 Signaling: Therapeutic Implications for ErbB2-Overexpressing Breast Cancers. *Cancer Res.* **2006**, *66*, 1640–1647. [[CrossRef](#)]